ASSESSMENT OF PRESENT ELECTROMAGNETIC TECHNIQUES FOR THE LOCATION OF TRAPPED MINERS

John Durkin
U.S. Department of Interior
Bureau of Mines
Pittsburgh Research Center
Pittsburgh, PA 15236

ABSTRACT

Field studies have been conducted in a large number of coal mines throughout the U.S. to determine the effectiveness of electromagnetic techniques in locating men trapped underground following a mine disaster. Data from these tests have been used to generate models of expected signal and noise distributions as found above mines throughout the coal fields. These distributions have aided in placing the expected performance of a through-the-earth electromagnetic communications technique into a probabilistic framework. Results indicate an expected 45% probability of detecting a miner's signal from a depth of 1,000 ft, a depth which exceeds 90% of the coal mines within the U.S. and a 90% probability at a depth of 500 ft, a depth which exceeds 50% of the mines.

INTRODUCTION

Following the Farmington mine disaster in 1968, the Bureau of Mines contracted with the National Academy of Engineering (5)* to recommend means to increase the probability of survival and rescue of miners in mine disasters. Their report recommended that the Bureau develop new communication techniques to detect and locate trapped miners. The Bureau considered these recommendations as the starting point for a continuing concentrated research effort to improve survival and rescue capability.

The condition of a mine after a disaster is unpredictable, cables may be cut and passages blocked. A hardened communication system that advances with the working face would be prohibitively expensive and might be inoperative when needed. Detection and communication with miners trapped underground requires signaling from the surface through the mine workings or directly through the strata.

---

* Number in parentheses refer to items in the list of references at the end of this paper.

Two major areas in rescue communications have been investigated: (a) Electromagnetic (EM) and (b) seismic. This paper examines the potential effectiveness of the EM signaling system and is particularly concerned with the statistical analysis of experimental magnetic field strength data taken at 94 coal mine sites well distributed over the U.S. coal fields. The objective of these tests was a data gathering venture intended to provide the necessary information for studies of probable effectiveness of the EM signaling system prior to initiating the formulation and promulgation of new regulations bearing on the use of such a system.

During the last decade theoretical studies and field tests indicated that the best chance of success rested in a system that consisted of an underground narrowband transmitter and a surface receiver, either used in a helicopter or hand carried by surface personnel, that would both detect the signal and locate its origin. Figure 1 illustrates the principle of operation of the EM trapped miner signaling device and associated surface receiving hardware. The transmitter and receiver were developed by Collins Radio.* (1) An improved version has recently been built by General Instrument Corp. (GI) (3) and is shown in Figure 2.

In practice, the miner would attach the belt-worn transmitter to a cap-lamp battery and deploy 300 ft of #18 copper wire around a coal pillar, ideally in a square configuration. If he cannot deploy the loop around a coal pillar, it can be deployed along a passageway where attempts are made to maximize the loop area. The transmitter delivers to the loop a pulsed square wave voltage of 630, 1050, 1950, or 3030 Hz of 100 ms duration and a 10% duty cycle. The established EM field is then detected by surface personnel. Once the signal is detected, the surface crew deploys a large loop of wire coupled to a high power audio amplifier that can be used for transmitting voice communications to the trapped miner. The underground transmitter contains a baseband receiver to receive the voice signals from the surface, and the miner can respond in code by keying the transmitter off and on. Figure 3 shows the life expectancy of the cap-lamp battery when operating the transmitter. The range of values was obtained when using an old battery with 8 hr discharge to an upper bound where a new battery with no discharge was used. A 2-ohm resistance was used as a load on the transmitter for these results. From this it can be seen that the transmitter can be expected to operate from approximately 2 to 4 days.

The objective of the field tests was twofold: First, to define a signal transmission measurement and analysis program to obtain a reliable data base for characterizing the signal transmission properties of overburdens in the U.S. coal fields; and second, to use this data base to predict the likelihood of successful performance of the EM trapped miner signaling

---

* Use of brand names is for identification purposes only and does not imply endorsement by the Bureau of Mines.

system. The mines sampled for these tests were selected from a population of all coal mines on the basis of both the overburden depth and the number of miners employed at the mine. The sample reflected concern both for for the physical dependence of signal penetration on depth and the number of miners exposed to potential disasters within each depth interval. Figure 4 shows the cumulative distribution of mines as related to the maximum depth and demonstrates that approximately 90% of the coal mines within the U.S. are less than 1,000 ft deep. These tests were performed by Westinghouse (8) and Bureau personnel. The analysis of the data as presented in this paper was performed by personnel of Arthur D. Little Inc. and the Bureau; details of this work can be found in an excellent report by Lagace et al. (4)

EARTH TRANSMISSION LOSS

In order to predict the surface signal level as produced from an underground transmitter, it is necessary to understand the expected loss the signal incurs when transmitted through-the-earth. Unfortunately, the geological structure of the overburden above coal mines differs from mine to mine which gives rise to differing electrical conducting properties. Therefore, for a given mine depth it can be expected that signal transmission characteristics will vary significantly from mine to mine. Consequently, one must rely on statistical information of the earth's transmission loss. A major objective of the 94-mine field test was to obtain enough data of the earth's transmission loss, as found over a large population of coal mines, to confidently characterize expected signal loss from an underground transmitter.

To ensure success in obtaining these data during the field tests, magnetic moments of the underground transmitter were used that were artificially higher than would be expected from a transmitter to be used by a miner. Therefore, in most cases, an earth transmission loss value for each mine was obtained. A strategy could then be formed to predict the expected surface signal strength based upon a given magnetic moment.

The RMS values of the vertical magnetic field, Hz, of all of the data taken were normalized to a transmitter magnetic moment of M = 1 Amp-m^2. Since the surface field is proportional to the magnetic moment of the underground transmitter, the expected level of the surface field for a given transmitter could then be found by accounting for the actual moment used. Following this normalization, statistical studies were performed to relate the surface field strength and mine depth at each frequency tested.

Each normalized data point can be denoted as S_{ij}, where the subscript i represents the specific frequency and the subscript j represents the specific depth of test for each mine. Thus, each surface measurement S_{ij} taken can be considered as a single observation of signal strength at a predetermined frequency and overburden depth level at a particular

mine. The selection of the mines tested was done on a statistically based random sample to assure that S_{ij} could be described by a common normal probability law.

Several linear regression models were hypothesized and tried. The model found to best fit the behavior of the data is one in which the mean value of the normalized signal strength S_{ij} is linearly related to the logarithm of overburden depth. This is shown in equation 1:

$$S_{ij} = \alpha_i + \beta_i \log (\text{depth}) + \varepsilon_{ij} \qquad (1)$$

Here S_{ij} is the normalized vertical magnetic field signal strength (expressed in dB re 1μA/m-RMS for the i th frequency and depth j for a transmit moment of M = 1 Amp-m^2.

The parameters α_i and β_i are parameters to be estimated from the data, where depth is known in meters. The parameter ε_{ij} represents a random variable that is normally distributed, with expected value zero and variance σ_{ij}^2 which is the same for all values of j.

The derived regression lines for each of the four frequencies are plotted in Figures 5-8. It is apparent visually that the log-linear relationship is an appropriate one and the R^2 statistic, a measure of goodness of fit, supports this observation.

Two types of intervals have been estimated from the data. One is known as a confidence interval, which is defined as a range of values computed from the sample that can be expected to include the true (but unknown) mean value with a known probability. Figures 9-12 display 95% confidence intervals with dashed lines. To illustrate this concept using Figure 9, it follows from the field experiment that the probability is 0.95 and that the interval from -6 dB to -12 dB includes the true mean normalized signal strength for a transmitter of magnetic moment M = 1 Amp-m^2 at 630 Hz and an overburden depth of 190 ft.

While the confidence interval represents a probability statement about a mean value over many trials, it is also of interest to quantify the expected outcome of a single trial. For example, what signal strength could be expected if a test were conducted at a predetermined frequency and overburden depth? This situation is depicted by prediction intervals also plotted in Figures 9-12. To illustrate this concept, again using Figure 9, the probability is 0.95 that another test performed at 630 Hz at a depth of 500 ft would yield a signal strength between -49 dB and -22 dB. Also plotted in Figures 9-12, for comparison, is a curve of the free space vertical field strength that would be measured on the surface in the absence of the lossy overburden media.

Figure 13 summarizes the normalized average overburden response as a function of depth and frequency by plotting the four regression lines and the free space curve on one graph. This figure shows that the frequency dependence of signal strength is relatively insignificant for depths

less than 500 ft, and that the change across the band is only about 10 dB even at the maximum depth of 1500 ft.

These summary normalized overburden response plots, together with the confidence and prediction levels of this section, can be used to generate estimates of signal strength produced on the surface above coal mines as a function of overburden depth and operating frequency for transmitters having any prescribed magnetic moment versus frequency characteristics in the 630 to 3030 band. This is assuming for a fixed magnetic moment, the size of the transmitting loop has no influence on the surface field.

GENERAL INSTRUMENTS TRANSMITTER

Using the results of the previous section on earth transmission loss statistics, the expected surface signal strengths produced by the recently developed GI transmitter can be predicted by computing the expected magnetic moment at each frequency and then translating each of the overburden response curves of Figure 13 upwards by an amount equal to the values of the magnetic moment expressed in dB re to 1 Amp-m^2.

The GI loop antenna consists of 300 ft of #18 copper wire, arranged in the shape of a square. This loop configuration was chosen because it best represents the practical implementation of the strategy that the miners will be instructed to follow. Figure 14 shows the predicted surface field strength when the GI transmitter is used. Also shown are the expected magnetic moments for each frequency.

SURFACE EM NOISE

Two independent sets of magnetic field noise measurements were obtained during the course of the measurement program. The first was by Westinghouse using the Collins' man-carried receiver. This set of data was found to be in error due to intramodulation problems caused by the simultaneous measurement of discrete man-made noise and broadband noise. The second set of data was obtained by a Bureau team performing similar tests at 27 of the mines tested. The Bureau's data were gathered on tape and later analyzed in the laboratory.

For purposes of signal detectability, the RMS value of the vertical magnetic field is of interest. The statistical distribution of this noise, using the Bureau data base, at each frequency for a receiver bandwidth of 30 Hz is shown in Figures 15-18.

SURFACE SIGNAL-TO-NOISE RATIO

In the previous sections, the behavior of signal data and noise data obtained in this study have been characterized by statistical relationships. To develop an understanding of detection probability it is necessary to characterize the probability distributions of the surface RMS signal-to-noise ratio (SNR) at each frequency.

The independence of signal and noise distributions, in addition to the property of normality exhibited by each distribution, permit straightforward combination of the two distributions to generate SNR probability estimates. By the central limit theorem the sum (or difference) of two normally and independently distributed variables is also normally distributed.

The SNR distributions are conveniently plotted using normal probability paper. This paper is designed so that the mean is plotted at the 50 percentile point and the mean plus or minus one standard deviation is plotted at the 16 or 84 percentile point, respectively. Such normal probability plots derived are given in Figures 19-22 for five different overburden depths at each of the four frequencies.

These four figures provide a straightforward method to estimate the probability of having various SNR in actual practice. The vertical axis represents the area under the normal curve from minus infinity to some SNR R_o and provides the probability of achieving a SNR less than or equal to R_o.

It is instructive to observe the behavior of probability estimates associated with exceeding a given SNR as a function of overburden depth and frequency. Figure 23 gives the probability of the RMS signal being at least greater than RMS noise. Note that the best performance occurs in the upper part of the frequency band even though more loss occurs through-the-earth at the higher frequencies and the magnetic moment is smaller at the higher frequencies. This can be explained due to the rapid decrease in surface noise level as frequency increases.

SIGNAL DETECTION CRITERIA

The success of a rescue effort when using a trapped miner transmitter rests on the ability of surface personnel to confidently detect the signal from the underground transmitter. The pulsed signals from the underground transmitters are detected by searchers carrying rescue receivers equipped with a handheld loop antenna and headsets. The mode of detection is aural, based on the headset signals perceived by the ear. It is then necessary to establish a relationship between the nature of the signal, SNR, and the probability of aural signal detection.

The aspects of the signal that influence detection are (a) frequency (b) signal length, and (c) signal repetition. The primary aspect of the noise for detection considerations, besides the level of the noise, is the noise bandwidth. How each of these parameters affects the signal detection capability must be understood, then their results can be combined to generate a probability of detection curve as a function of SNR.

The present receiver mixes the received signal with an internal oscillator to a higher frequency for purposes of narrowband filtering, then mixes the filtered signal again to present a listening signal of 978 Hz to the operator. The ability to detect a tone masked by broadband noise as a function of frequency has been studied by Urick (7).

In this work, an entity known as critical bandwidth evolved. When the ear listens for a tone it acts as a narrowband filter centered at the signal frequency. The masking of the signal by the noise will only be influenced by the noise within this critical band. Noise outside this band will have no influence on signal detectability. Figure 24 illustrates the critical bandwidth values as a function of frequency and shows that the critical bandwidth is approximately 60 Hz at the 978 Hz listening frequency of the rescue receivers.

The effect of the length of a pulsed tone is shown in Figure 25. Psychoacoustic data taken by a number of investigators are combined in this figure to show the "recognition differential" required versus pulse length for a 50% probability of detection. The recognition differential is the amount in dB by which the signal level needs to exceed the measured noise spectrum level (noise level in 1 Hz within critical band of interest) to provide a 50% probability of detection.

The GI transmitters have a fixed pulse duration of 100 ms which prescribes a recognition differential of 23 dB to achieve a 50% probability of detection. To determine the significance of the 23 dB recognition differential in terms of required SNR, a bandwidth must be chosen. The bandwidth used in the receiver is 30 Hz, one-half of the critical bandwidth of the ear at the listening frequency. It is assumed here that the noise reaching the operator's ear is produced solely by the receiver and that the attenuation provided by the headset is sufficient to justify disregarding ambient acoustic noise in the area of the operator. Studies (6) have shown that systems with bandwidths approximately one-half the critical bandwidth will behave in the same manner detection-wise as those having a system bandwidth equal to the critical bandwidth. Therefore, for purposes of the trapped miner system, a SNR of 23 -10 log 30 = 8 dB is needed to yield a 50% probability of detection.

A final factor affecting detection is the signal repetition rate. Garner (2) provides data on the effect of the repetition of a pulsed tone on signal detectability. Figure 26 illustrates these findings. This work shows that as the repetition rate of a 50 ms pulse of a 1000 Hz signal is changed from 1 in 4 seconds to 1 per second, 2 dB less SNR is required. Reviewing Garner's data would indicate that an even greater improvement might be expected for the trapped miner transmitter, but the lack of data at repetition rates less than 1 per 4 seconds precludes a guarantee of this. Therefore, a conservative 2 dB improvement value will be used. The 50% probability of detection SNR criterion of (8-2) dB or 6 dB, will be used.

This work quantifies the necessary SNR to establish a 50% detection probability. It is also necessary to extend this work to determine detection probabilities at any other SNR. The results of this extension are shown in Figure 27. This plot can be used with the earlier established expected SNR for the underground GI transmitter to establish signal detection probabilities.

PROBABILITY OF DETECTION ESTIMATES

In an actual mine emergency situation many factors will influence the actual ability to rescue the miner. Time of arrival of the rescue team, life expectancy of the miner, search times, and operation time of the underground transmitter are only a few of the factors that have a bearing on the success of the rescue effort. This report has not discussed these points but rather has investigated the detection probability for an existing signal as being measured by a rescue team in an area which in general is directly over the trapped miner. Even within this measurement there are factors such as geology, noise, and depth that influence the probability of success. However, though these factors may not enable us to state the success of this measurement in a deterministic manner, we can, as outlined in this paper, quantify our chances in a probabilistic framework.

The probability of detection curve in Figure 27 actually represents a conditional probability; that is, the likelihood that detection will occur given the presence of a fixed RMS SNR. As a consequence, the chance of detecting a signal transmitted through the earth can be calculated according to:

$$P\{D \text{ and } R_k\} = P\{R_k\} \times P\{D|R_k\} \tag{2}$$

where $P\{D \text{ and } R_k\}$ represents the probability of achieving a SNR of size R_k and also detecting the signal embedded in the noise. $P\{R_k\}$ is the probability of the occurrence of a SNR of size R_k and $P\{D|R_k\}$ is the conditional probability of detecting a signal given a SNR of size R_k.

Figure 27 gives $P\{D|R_k\}$, and Figures 19-22 show the SNR probability distributions. The latter figures show that these probabilities depend on frequency and depth. Using additional subscripts to account for these parameters, the probability of achieving a SNR of size R_k and detecting the signal transmitted from a depth i at frequency j is

$$P_{ijk}\{D \text{ and } R_k\} = P_{ij}\{R_k\} \times P\{D|R_k\} \tag{3}$$

However, the primary result is the expected probability of detecting a signal transmitted at a specified depth for a known frequency summed over all possible R_k's. This is given as

$$P_{ij}\{D\} = \sum_{R_k} P_{ijk} \tag{4}$$

The results of these calculations present, as shown in Figure 28, the expected property of detection estimates for the GI transmitter signals as measured over all the U.S. coal fields.

SUMMARY

This paper has discussed the results of an extensive field testing program to evaluate the performance of the EM trapped miner transmitter. Analysis of these data has enabled one to place into a probabilistic framework the ability to confidently detect the signal from the underground transmitter. Results indicate that the probability of detecting this signal is 45% at a depth of 1,000 ft, a depth which exceeds 90% of the mines within the U.S. and a 90% probability at a depth of 500 ft, a depth which exceeds 50% of the mines. This information is vital for the future formulation and promulgation of new regulations written for the use of the EM system. Studies are currently underway to improve the detection capability by providing signal processing capability to the receiver. Future work will look at a systems approach when using this technique. This study will investigate each element involved in a successful rescue effort, such as search strategies, life expectancies, etc. Coupled with the results discussed in this paper, a thorough understanding of the effective implementation of the EM system will be obtained.

REFERENCES

1. Collins Radio, "Waveform Generator--Package and Receivers," USBM, Final Report, Contract H0242010.

2. Garner, W. R., "Auditory Thresholds of Short Tones as a Function of Repetition Rates," JASA, vol. 19, No. 4, July 1947, pp 600-608.

3. General Instrument Corporation, "Design to Specification and Fabrication of VF Transmitters and Baseband Receivers," USBM contract J0395017.

4. Lagace, R., J. Dobbie, T. Doerfler, W. Hawes and R. Spencer, "Technical Support of Through-the-earth Transmission Measurement Arthur D. Little, Inc., USBM contract J0188087, Final Report, June 1980.

5. National Academy of Engineering, Mine Rescue and Survival, Bureau of Mines, Open File Report 4-70, March 1970.

6. Principles and Applications of Underwater Sound, Summary Technical Report of Division 6, NDRC, vol. 7, Washington, D.C., 1946 (revised 1968).

7. Urick, R. J., "Principles of Underwater Sound for Engineers," McGraw-Hill, 1967.

8. Westinghouse, "Reliability and Effectiveness Analysis of the USBM Electromagnetic Location System for Coal Mines," USBM contract J0166060, Final Report, December 1978.

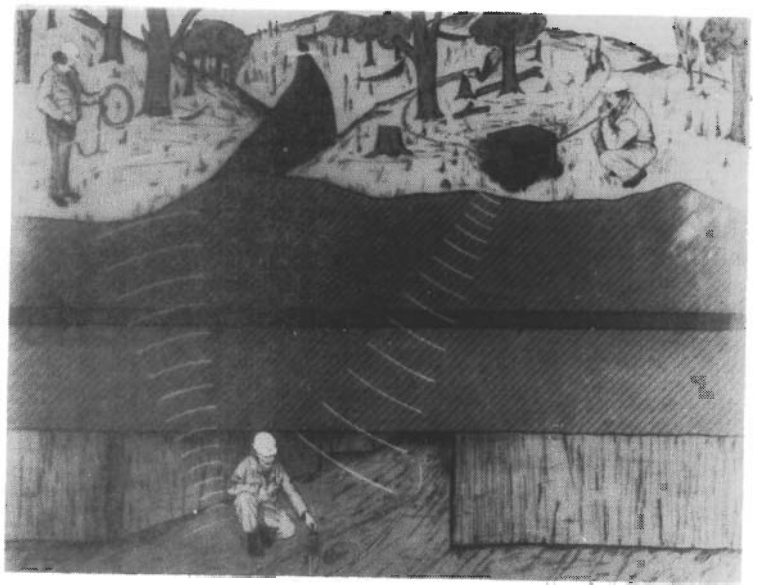

FIG. 1. Illustration of operation of trapped miner transmitter

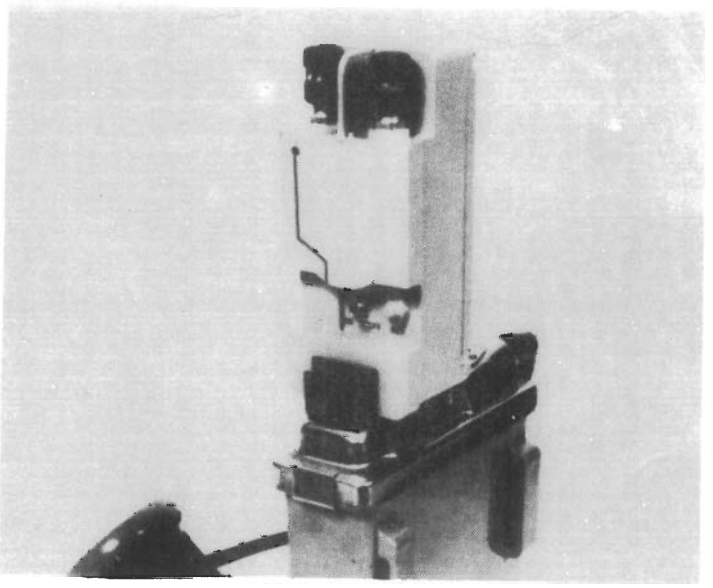

FIG. 2. Trapped miner EM transmitter with cap-lamp battery

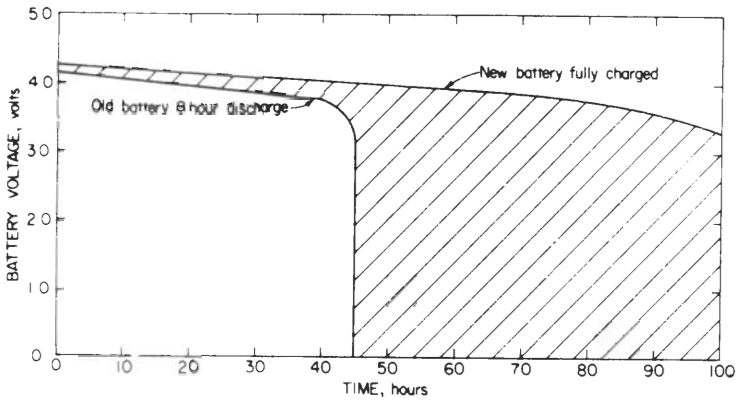

FIG. 3. Cap-lamp voltage variation with time while operating trapped miner transmitter

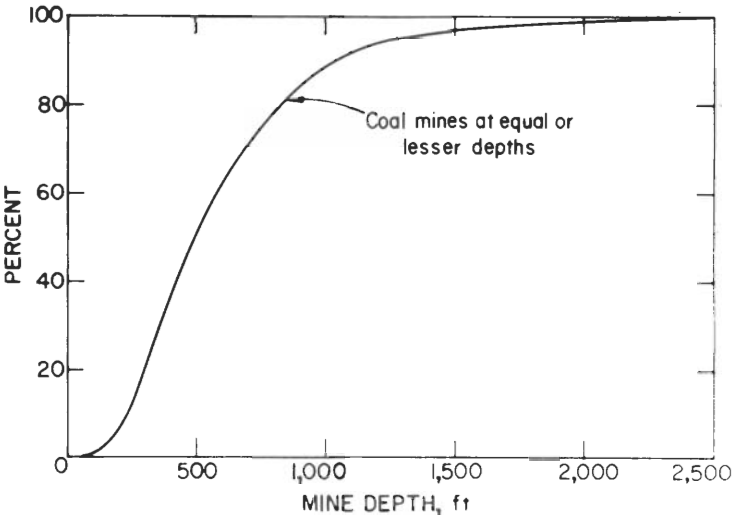

FIG. 4. Cumulative distribution of coal mine depths throughout the U.S.

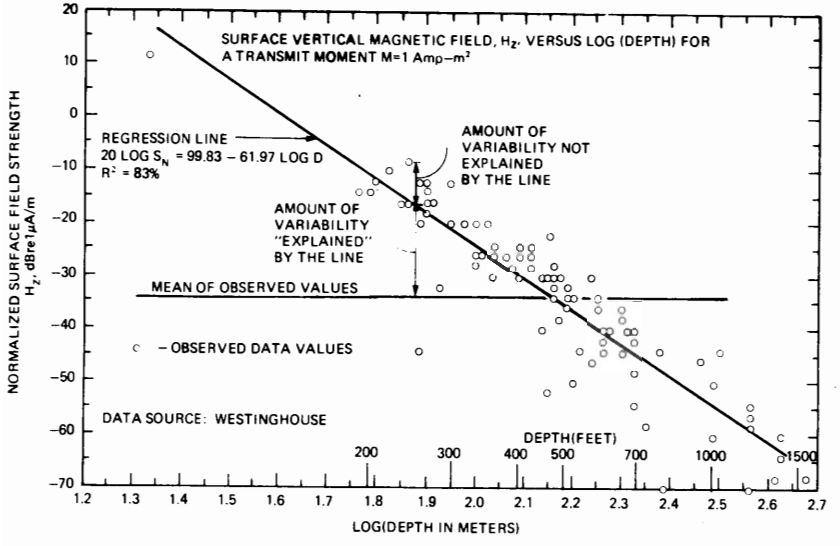

FIG. 5. Uplink normalized overburden signal response data and linear regression log (depth) model at 630 Hz.

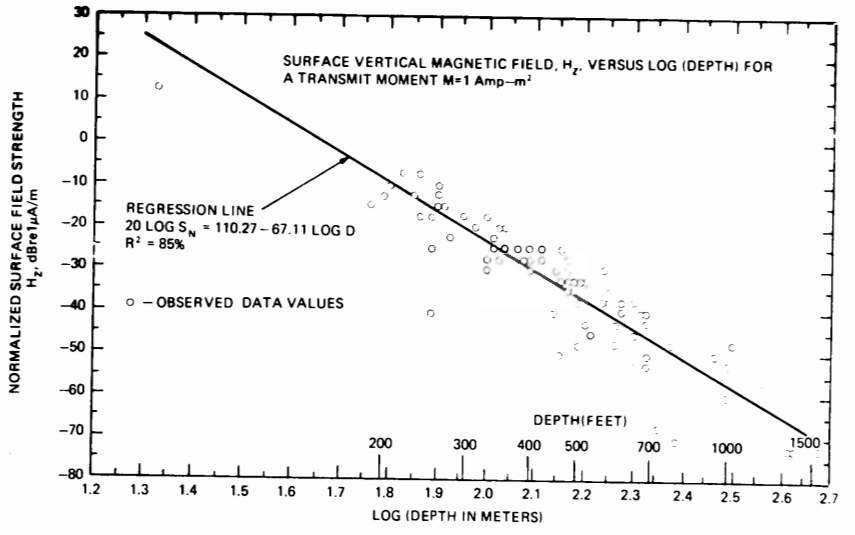

FIG. 6. Uplink normalized overburden signal response data and linear regression log (depth) model at 1050 Hz.

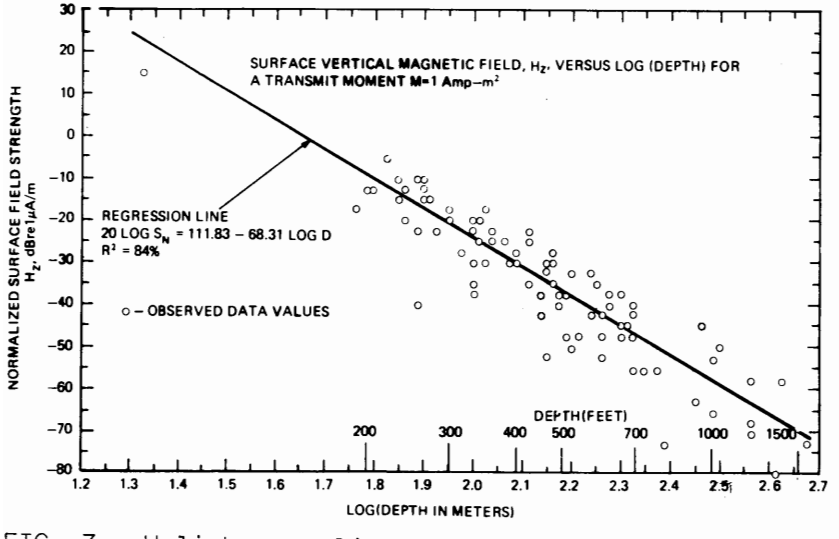

FIG. 7. Uplink normalized overburden signal response data and linear regression log (depth) model at 1950 Hz.

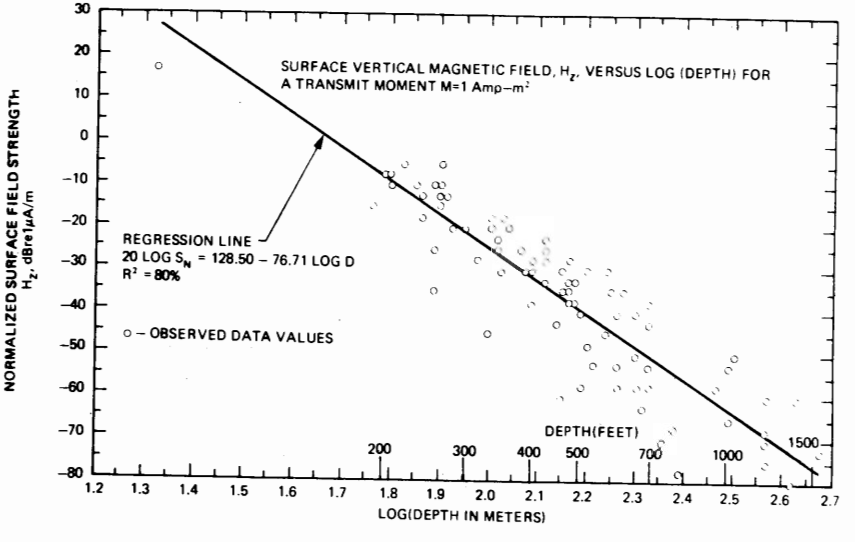

FIG. 8. Uplink normalized overburden signal response data and linear regression log (depth) model at 3030 Hz.

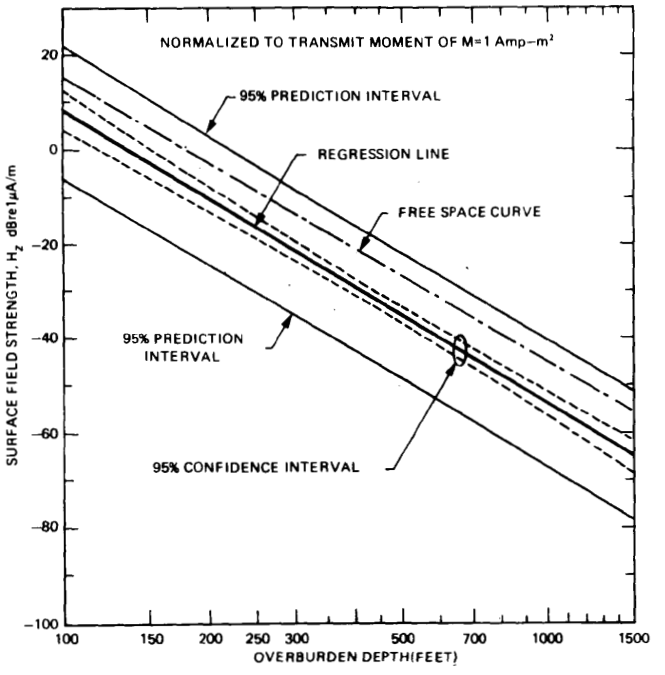

FIG. 9. Uplink regression results for 630 Hz normalized vertical signal strength, Hz, vs. depth.

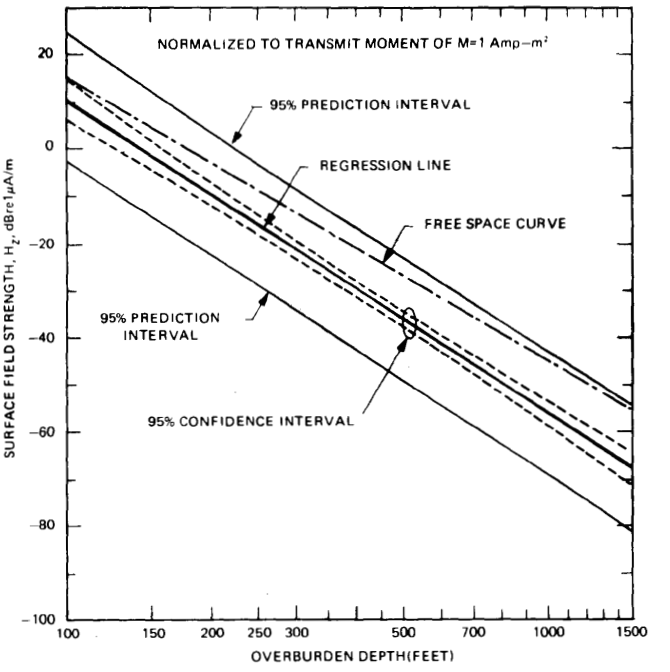

FIG. 10. Uplink regression results for 1050 Hz normalized vertical signal strength, Hz, vs. depth.

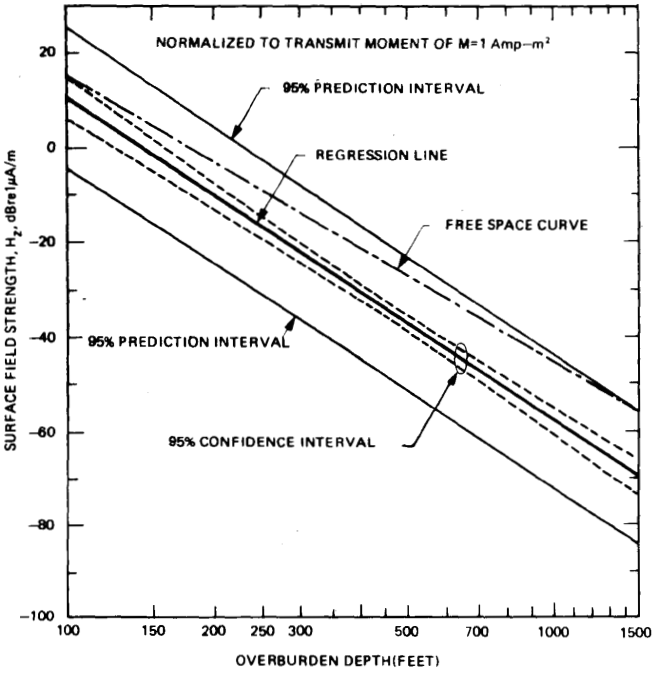

FIG. 11. Uplink regression results for 1950 Hz normalized vertical signal strength, Hz, vs. depth.

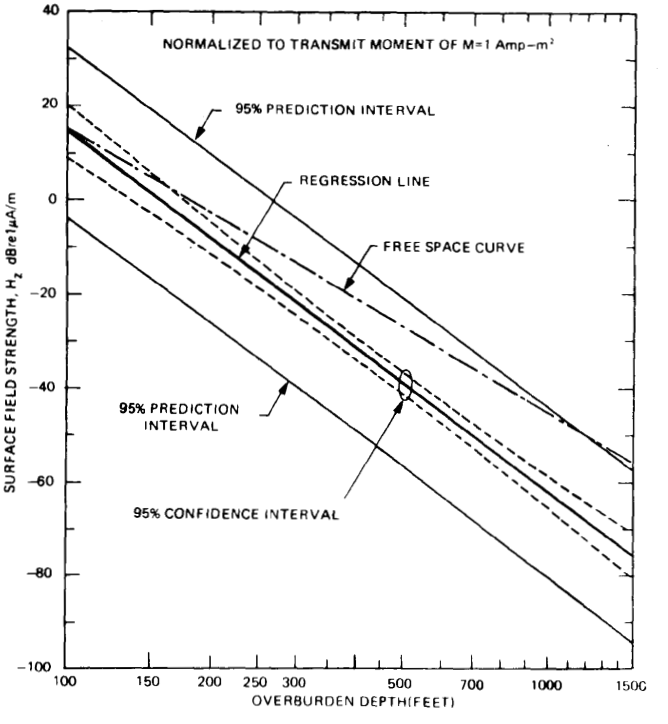

FIG. 12. Uplink regression results for 3030 Hz normalized vertical signal strength, Hz, vs. depth.

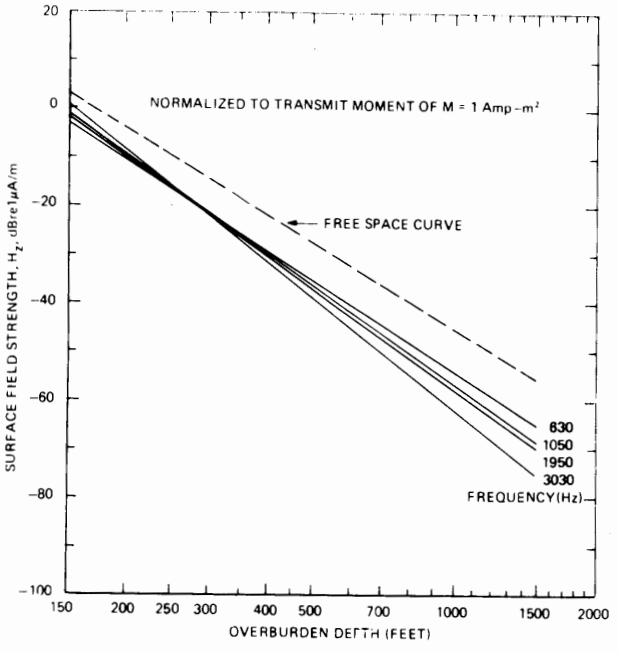

FIG. 13. Normalized overburden response curves--uplink regression results, average surface vertical signal strength, Hz, vs. overburden depth by frequency.

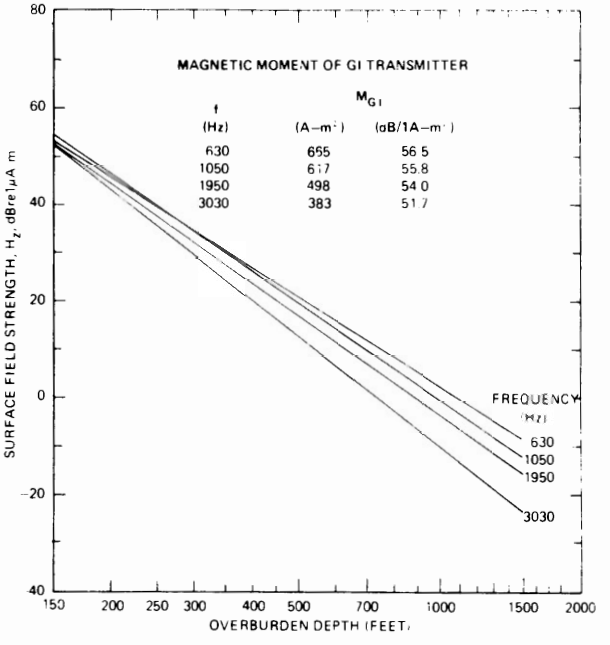

FIG. 14. Predicted uplink response curves for General Instruments transmitter--average surface vertical magnetic field signal strength, Hz, vs. depth by frequency.

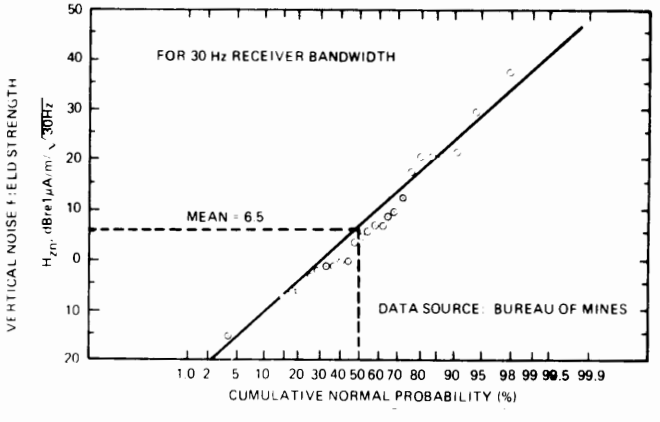

FIG. 15. Statistical distribution of RM surface noise at 630 Hz.

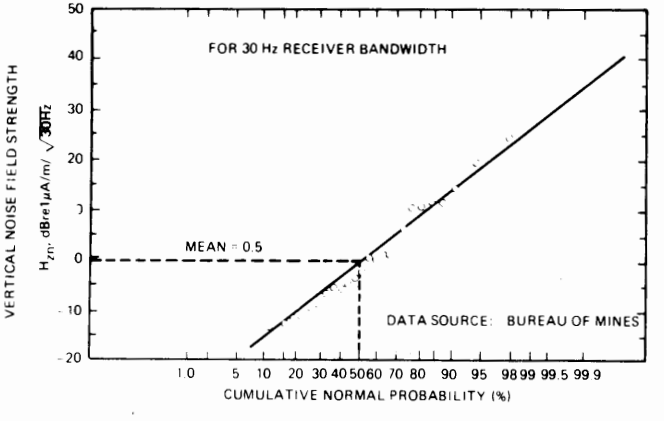

FIG. 16. Statistical distribution of RM surface noise at 1050 Hz.

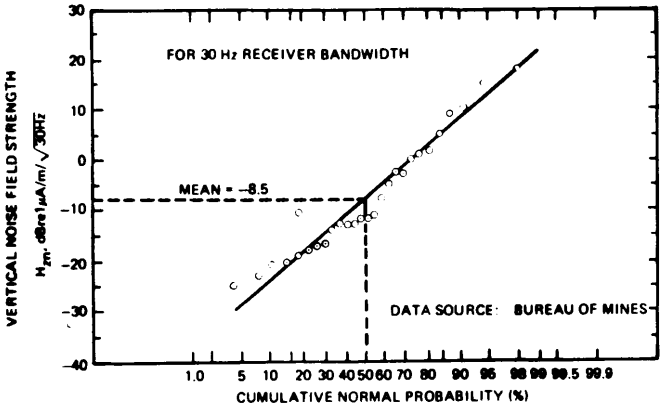

FIG. 17. Statistical distribution of RM surface noise at 1950 Hz.

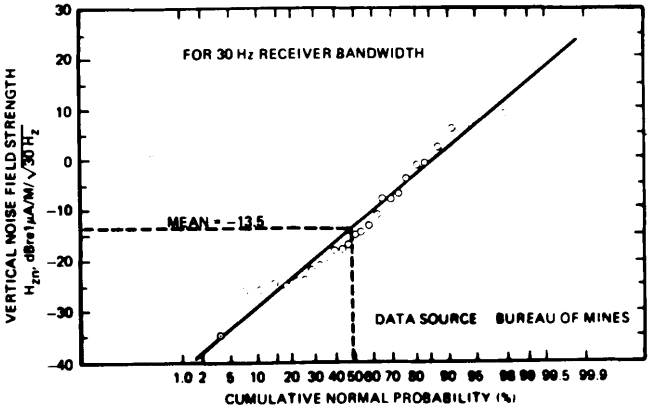

FIG. 18. Statistical distribution of RM surface noise at 3030 Hz.

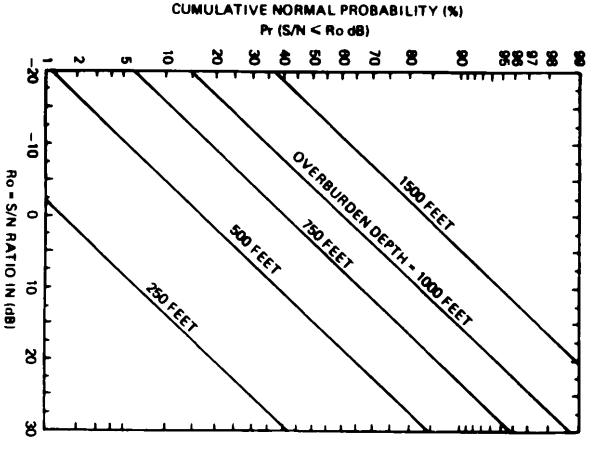

FIG. 19. Cumulative probability distribution of S/N ratios expected above U.S. underground coal mines at 630 Hz.

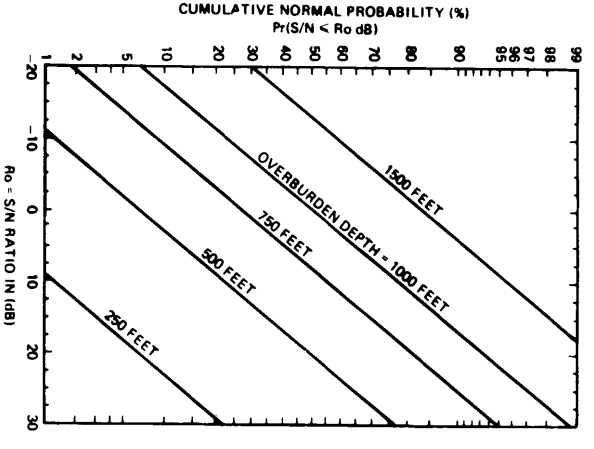

FIG. 20. Cumulative probability distribution of S/N ratios expected above U.S. underground coal mines at 1050 Hz.

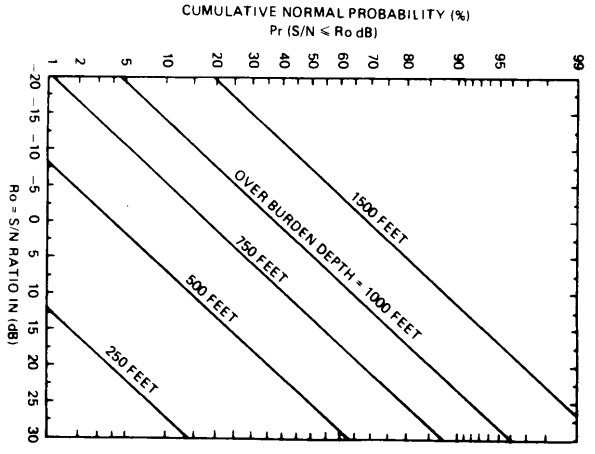

FIG. 21. Cumulative probability distribution of S/N ratios expected above U.S. underground coal mines at 1950 Hz.

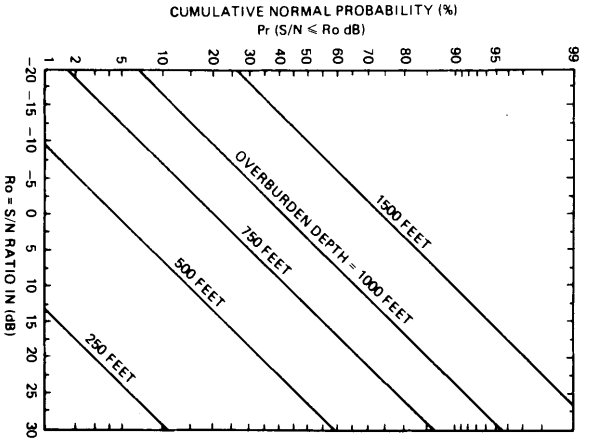

FIG. 22. Cumulative probability distribution of S/N ratios expected above U.S. underground coal mines at 3030 Hz.

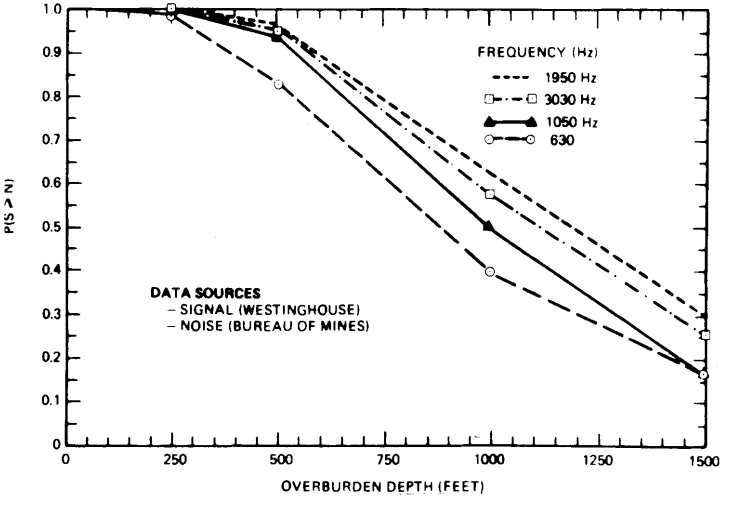

FIG. 23. Probability that mean RMS signal is greater than or equal to RMS noise + 9 dB for the General Instruments transmitter.

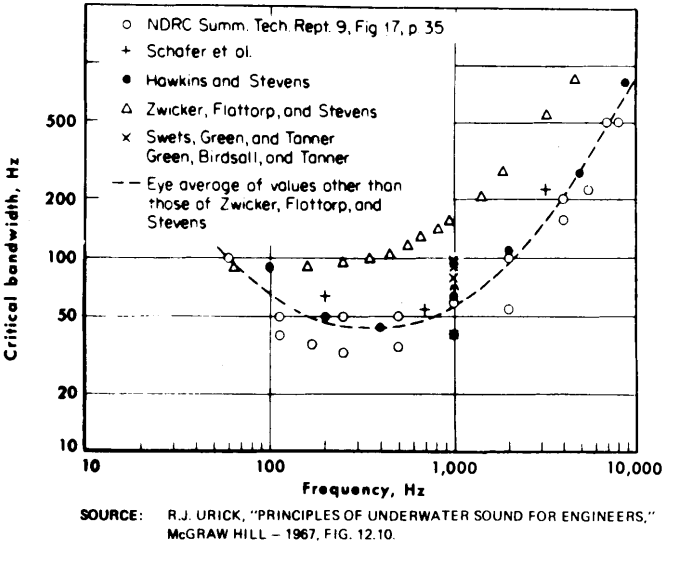

FIG. 24. Measured values of the critical bandwidth of the ear.

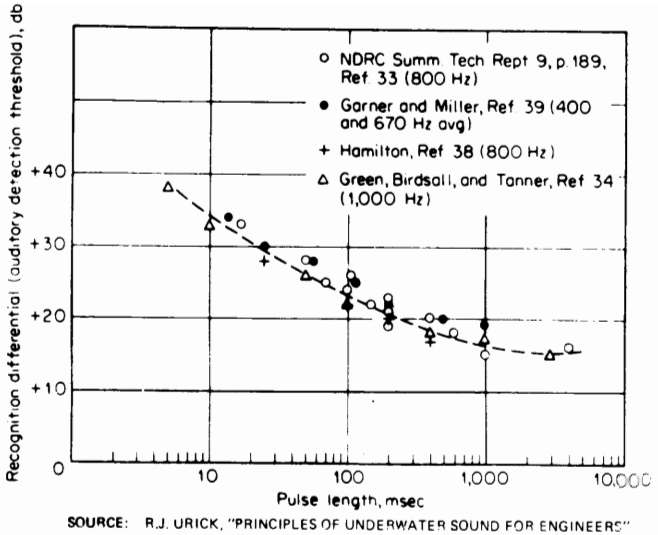

SOURCE: R.J. URICK, "PRINCIPLES OF UNDERWATER SOUND FOR ENGINEERS" McGRAW HILL–1967, FIG. 12.11.

FIG. 25. Recognition differential (auditory detection threshold, DT) for sinusoidal pulses in Broadband noise reduced to 1-Hz bands.

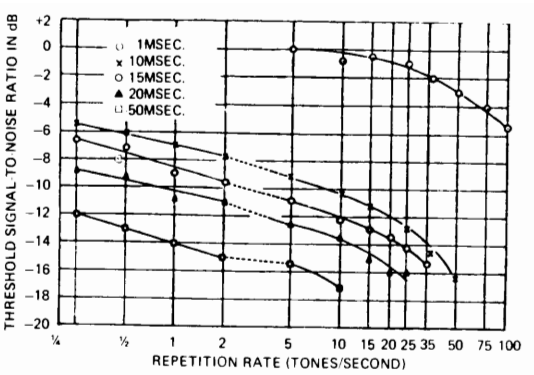

NOTE: EACH CURVE IS FOR A DIFFERENT TONAL DURATION. THE MASKING NOISE WAS FILTERED WITH A 5000 Hz LOW PASS FILTER, AND SIGNAL-TO-NOISE RATIOS ARE WITH RESPECT TO THE TOTAL NOISE ENERGY. THE INTENSITY OF THE MASKING NOISE WAS APPROXIMATELY 90 dB re 0.0002 dyne/cm². FREQUENCY IS 1000 Hz.

SOURCE: W.R. GARNER "AUDITORY THRESHOLDS OF SHORT TONES AS A FUNCTION OF REPETITION RATES", JASA VOL. 19, NO. 4, JULY 1947, PP. 600–608, FIG. 4.

FIG. 26. The effect of repetition rate of short tones on the masked threshold.

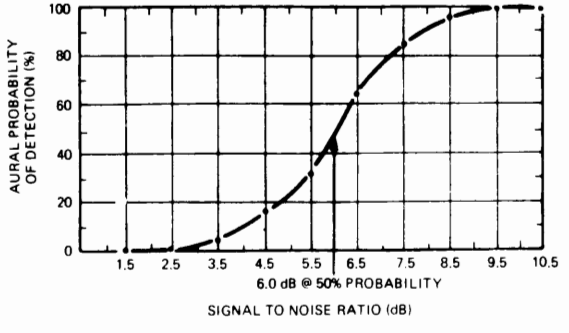

NOTE: FOR 100 MILLISECOND PULSES, 1 PER SECOND REPETITION RATE, 957 Hz LISTENING FREQUENCY, AND 30 Hz RECEIVER BANDWIDTH.

SOURCE: Arthur D. Little, Inc., and R.J. Urick.

FIG. 27. Aural probability of detection vs. RMS signal-to-noise ratio for trapped miner pulsed CW signals in background Gaussian noise.

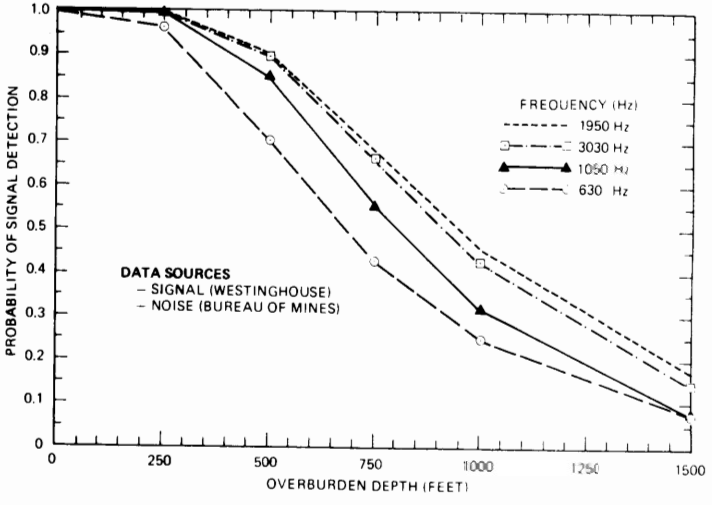

FIG. 28. Predicted probability of signal detection vs. overburden depth by frequency for the General Instruments transmitter.